AD-C010061

SECURITY REMARKING REQUIREMENTS

DOD 5200.1-R, DEC 78

REVIEW ON 01 JAN 97

CONFIDENTIAL

ADC010061

MAY 20

AD NO.
DDC FILE COPY

xonics

6849 HAYVENHURST AVENUE, VAN NUYS, CALIF. 91406

(213) 787-7380

CONFIDENTIAL

CONFIDENTIAL

EFFECT OF ARRAY TILT ON
BEAM NOISE, SIGNAL-TO-NOISE RATIO,
AND DETECTION OPPORTUNITY STATISTICS (U)

TR-109-OSD

1 January 1977

Prepared by:
Carl F. Morey

Prepared for:

Long Range Acoustic Propagation Project
Department of the Navy
Naval Ocean Research and Development Activity
Bay St. Louis, MS 39520

Under Contract N00014-77-C-0082

Xonics, Inc.
6849 Hayvenhurst Avenue
Van Nuys, California 91406
(213) 787-7380

Classified by OPNAVINST S5510.72C
Exempt from GDS of E.O. 11652
Ex. Cat (3); Declassified on
31 December 2007

NATIONAL SECURITY INFORMATION
Unauthorized Disclosure
Subject to Criminal Sanctions

CONFIDENTIAL

ABSTRACT (U)

(C) This study investigates the effect of array tilt on the statistics of noise clutter attributed to ships. In particular, the study calculates the statistics of beam noise, signal-to-noise ratio, and detection opportunities (zero ships on the beam) for a rigid line array of idealized beams without associated sidelobes and for idealized beam noise and signal models. The results are that:

- The variance of beam noise fluctuations and the probability of zero ships on the beam decrease with array tilt while the mean beam noise level is independent of array tilt;
- The variance of the signal-to-noise ratio fluctuations decreases with array tilt, while the mean signal-to-noise ratio is constant with array tilt; and
- The probability of detection opportunities decreases with array tilt and the mean waiting time between detection opportunities increases with array tilt, while the mean duration of detection opportunities is independent of array tilt.

(C) Consequently, the central conclusion of the study is that detection performance of a line degrades significantly as the line array tilts from the horizontal plane by small angles.

TABLE OF CONTENTS (U)

INTRODUCTION (U)

(C) Recent experimental evidence has shown that a towed line array will tilt with respect to the horizontal if not properly balanced for operating tow depth. Several studies have investigated the impact of tilt on various aspects of system performance. One of these, for example*, has calculated bearing error as a function of tilt and has concluded that for modest tilts ($< 5^0$) the performance of the broadside and near broadside beams in establishing target bearing is relatively insensitive to array tilt. However, other aspects of performance not only exhibit high sensitivity to array tilt but also differ from the case of bearing error in that degradation in performance cannot be corrected, even in principle, from knowledge of tilt magnitude. One of these aspects is the ability of a narrow beam towed line array to "look" between discrete shipping noise sources during which periods enhanced detection performance may be possible when the noise level approaches or achieves base noise levels.

OBJECTIVES (U)

(U) The objectives of this study are to determine the effects of array tilt on:

- o Beam noise statistics,
- o Signal-to-noise statistics,
- o Duration of detection opportunities (zero ships on the beam), and
- o Waiting time between detection opportunities,

using idealized array, noise, and signal models.

(U) Calculations were performed for the EASTPAC summer/fall, sound speed profile of Figure 1A. Limiting rays for deep sound channel propagation are shown as a function of depth in Figure 1B, where it can be seen that at the edge of the sound channel, the energy arriving via the deep sound channel propagation arrives at 0^0 (horizontal) and that at the axis of the sound channel (700 meters), the deep sound channel energy arrives within $\pm 15^0$.

*Watson, W. H., "LAMBDA Performance Analysis: Predicted Performance Degradation from Geometrical Array Distortion," Naval Undersea Center, 6 Jan 77

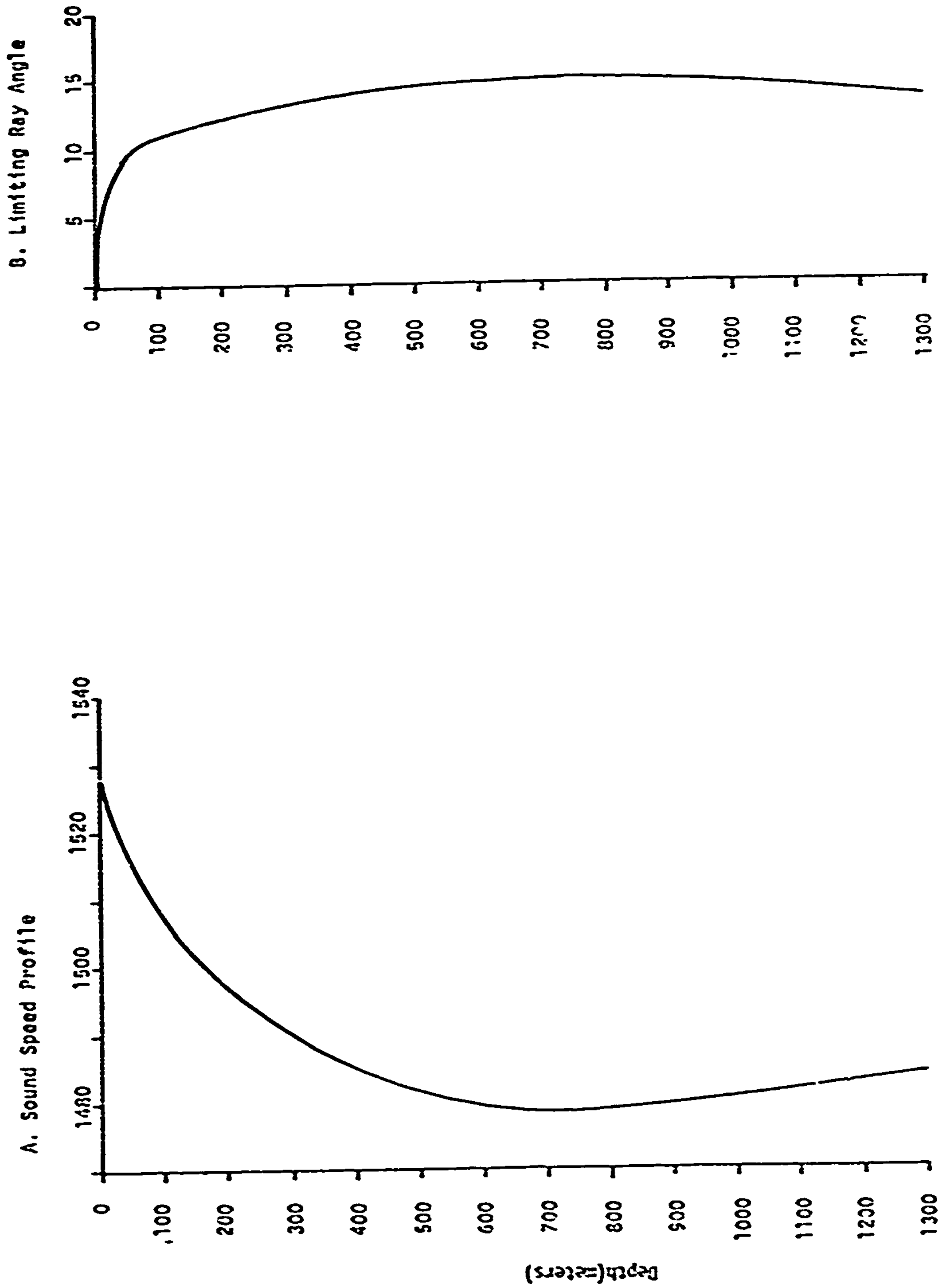

Figure 1. EASTPAC Summer/Fall Sound Speed Profile (U)

ARRAY MODEL (U)

(U) The array is modelled as a linear line array that tilts as a rigid body and forms ideal, cylindrically symmetrical beams without associated sidelobes, as shown in Figure 2.

(U) Figure 3 depicts the geometric centers of several beams in azimuth-elevation space for horizontal orientation of the array. Here, with the exception of the broadside (90^0) and endfire (0^0 and 180^0) beams, all beam azimuths vary with elevation angle. Thus, for signal arrivals close to horizontal, where azimuths do not vary significantly, a beam angle (together with array heading) can give a good indication of signal source bearing.

(U) Figure 4 shows the orientation of the Figure 3 beam centers when the array is tilted aft with respect to the horizontal. When the array tilts aft, forward beams are elevated, aft beams are depressed, and near broad-side beams look forward at some elevation angles and aft at others.

(U) Figure 5 shows that the near broadside beams of Figures 3 and 4 can be approximated by linear beams in azimuth-elevation space. Each of these beams spans an azimuth sector that is a function of array tilt angle and elevation angle approximately given by

$$\gamma = \theta + 2\alpha \tan \beta,$$

where

γ = azimuth sector,
θ = beamwidth,
α = elevation angles, and
β = array tilt angle

(U) Figure 6 shows the azimuth sector spanned by a 1^0 near broadside beam as a function of array tilt angle for elevation angles of $\pm 5^0$, $\pm 10^0$, $\pm 15^0$, and $\pm 20^0$.

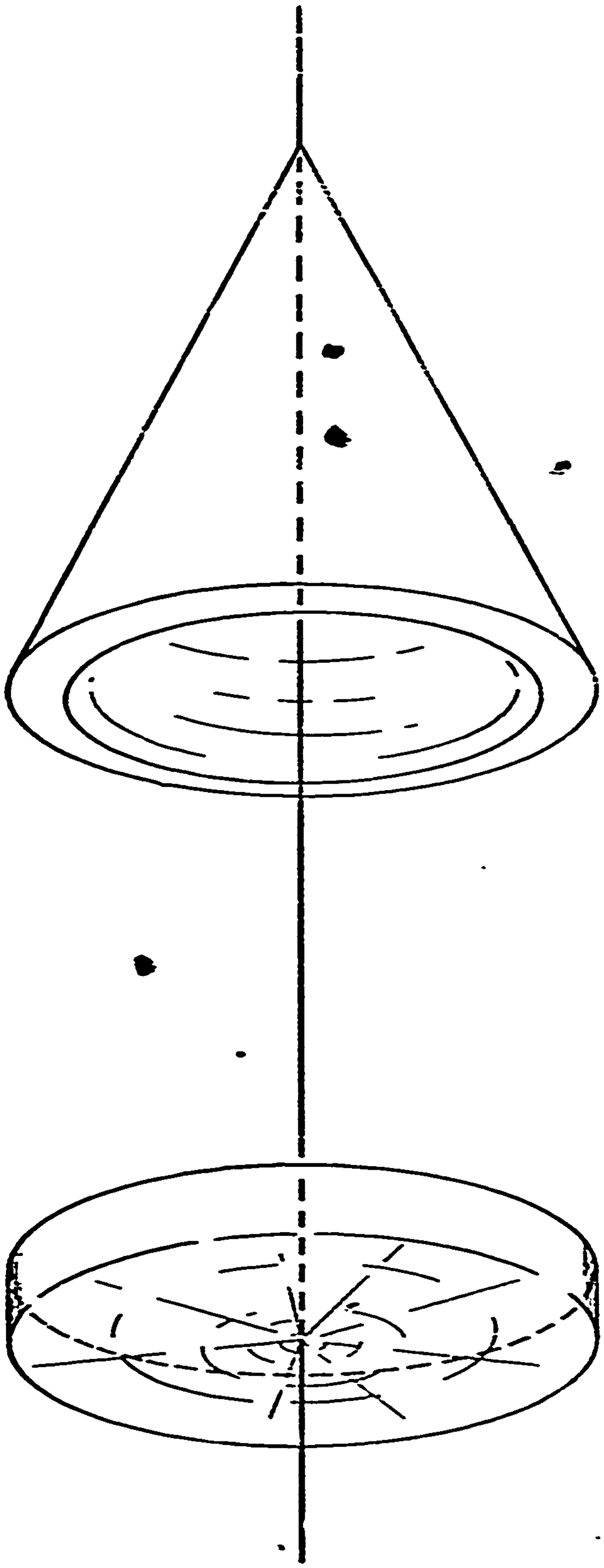

Figure 2. Typical Beams (U)

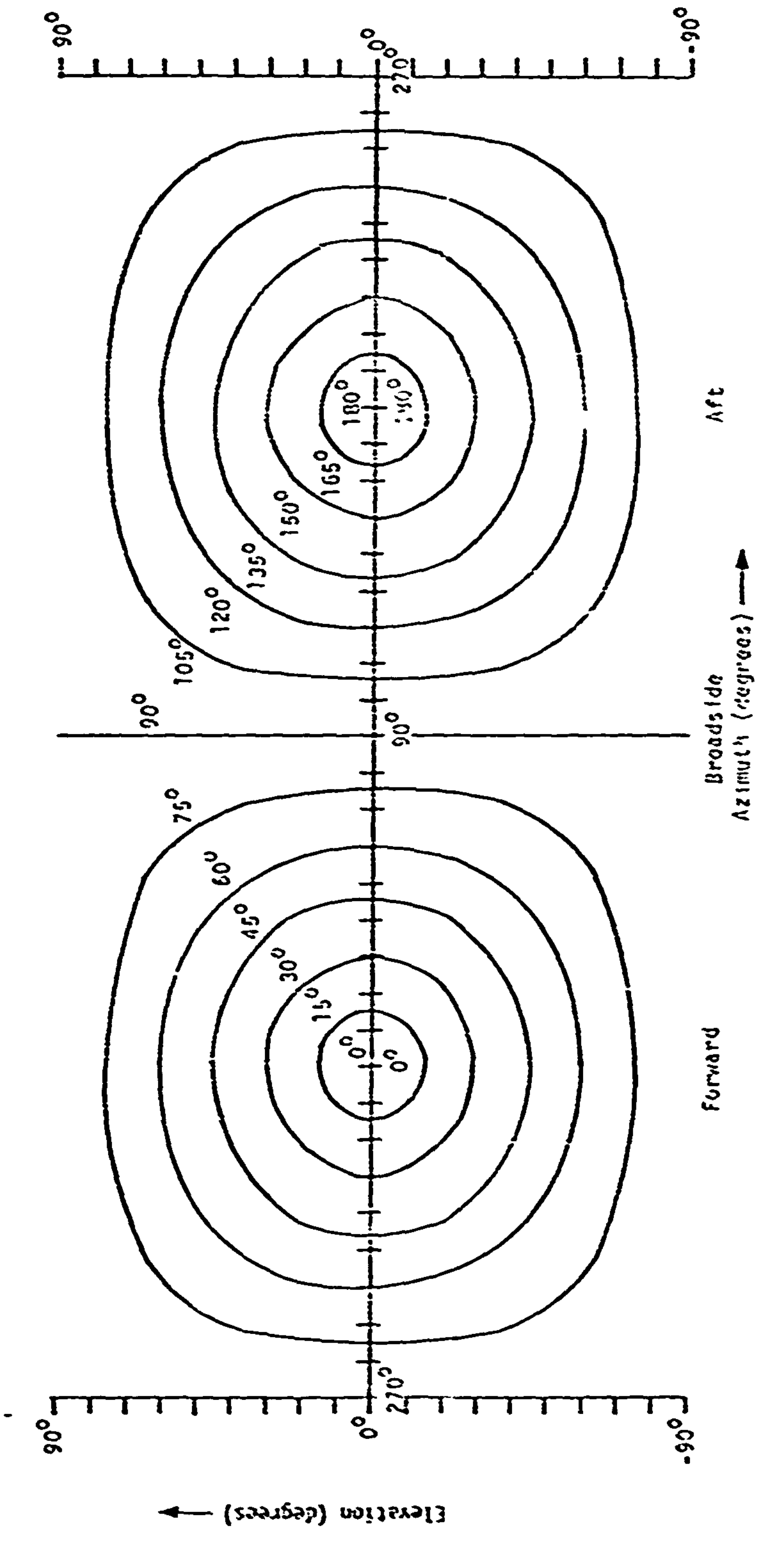

Figure 3. Beam Centers for a Horizontal Array (U)

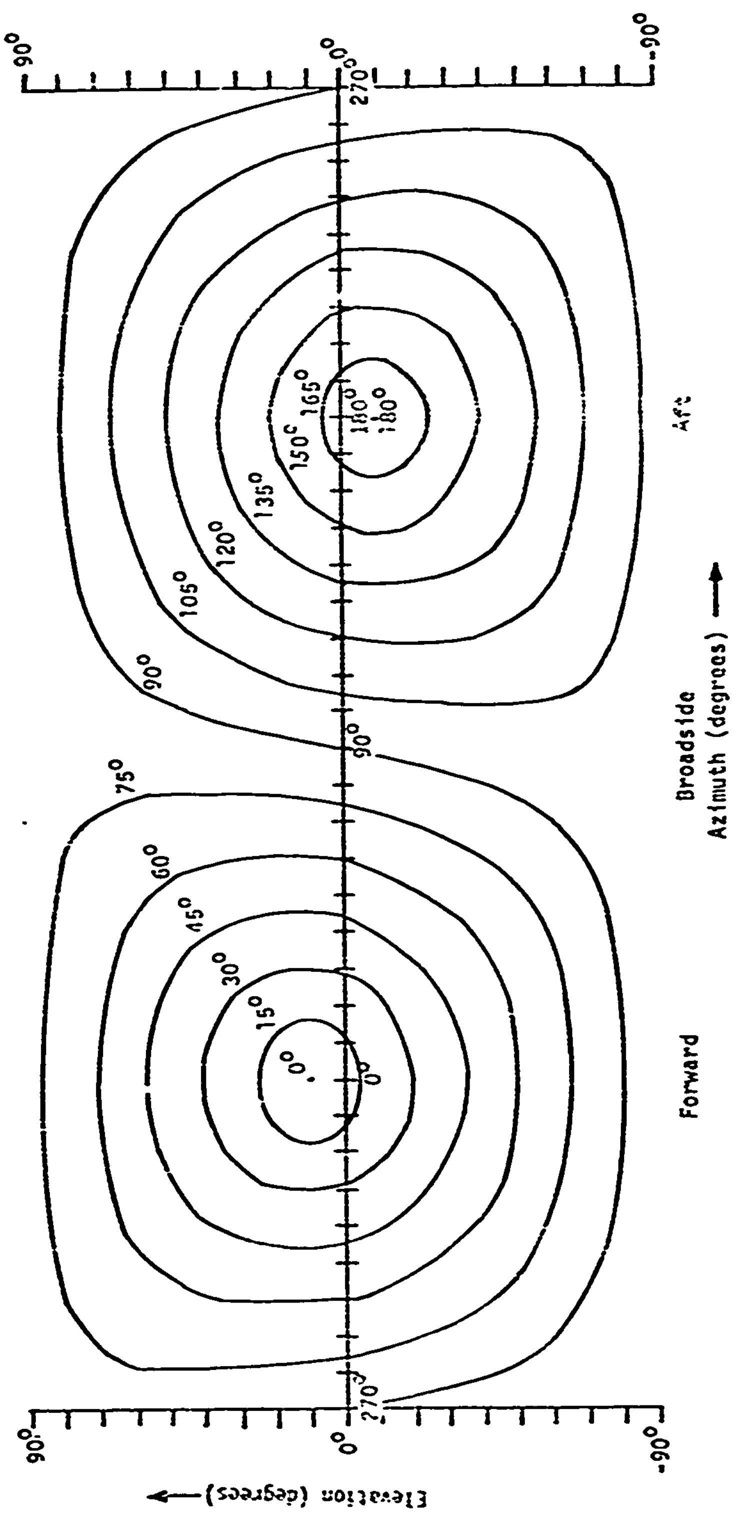

Figure 4. Beam Centers for an Array Tilted Down Aft (U)

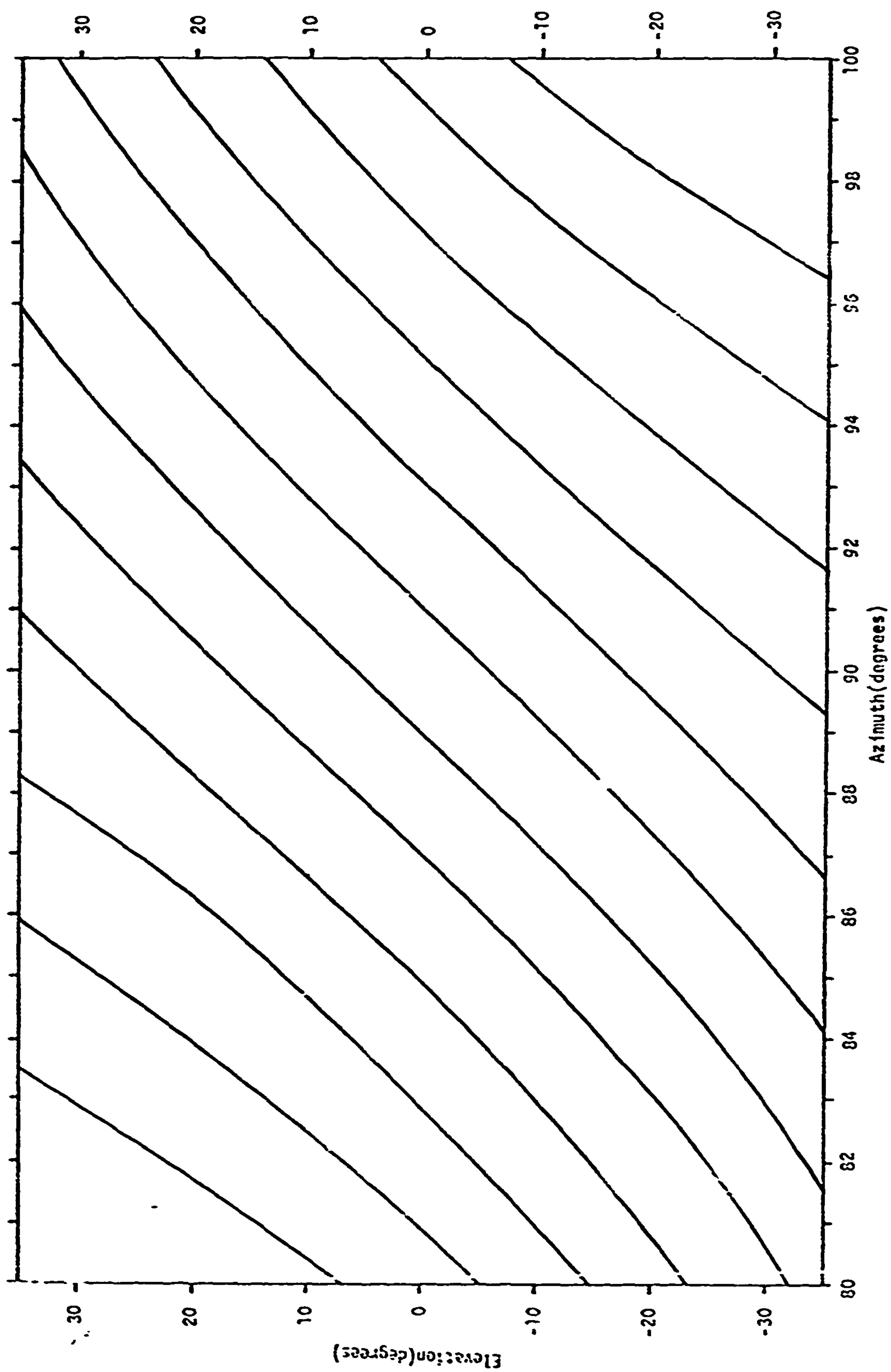

Figure 5. Near Horizontal Broadside Beams (U)

(U) Figure 5 shows that the near broadside beams can be approximated by linear beams in azimuth-elevation space. Each of these beams spans a sector of azimuth that is a function of array tilt angle and elevation angle. The azimuth sector is approximately given by

$$\gamma = \theta + 2\alpha \tan \beta$$

where

γ = azimuth sector

θ - beamwidth

α = elevation angles

β = array tilt angle

(U) Figure 6 shows the azimuth sector spanned by a 1^0 beam as a function of array tilt angle for elevation angles of $\pm 5^0$, $\pm 10^0$, $\pm 15^0$, and $\pm 20^0$.

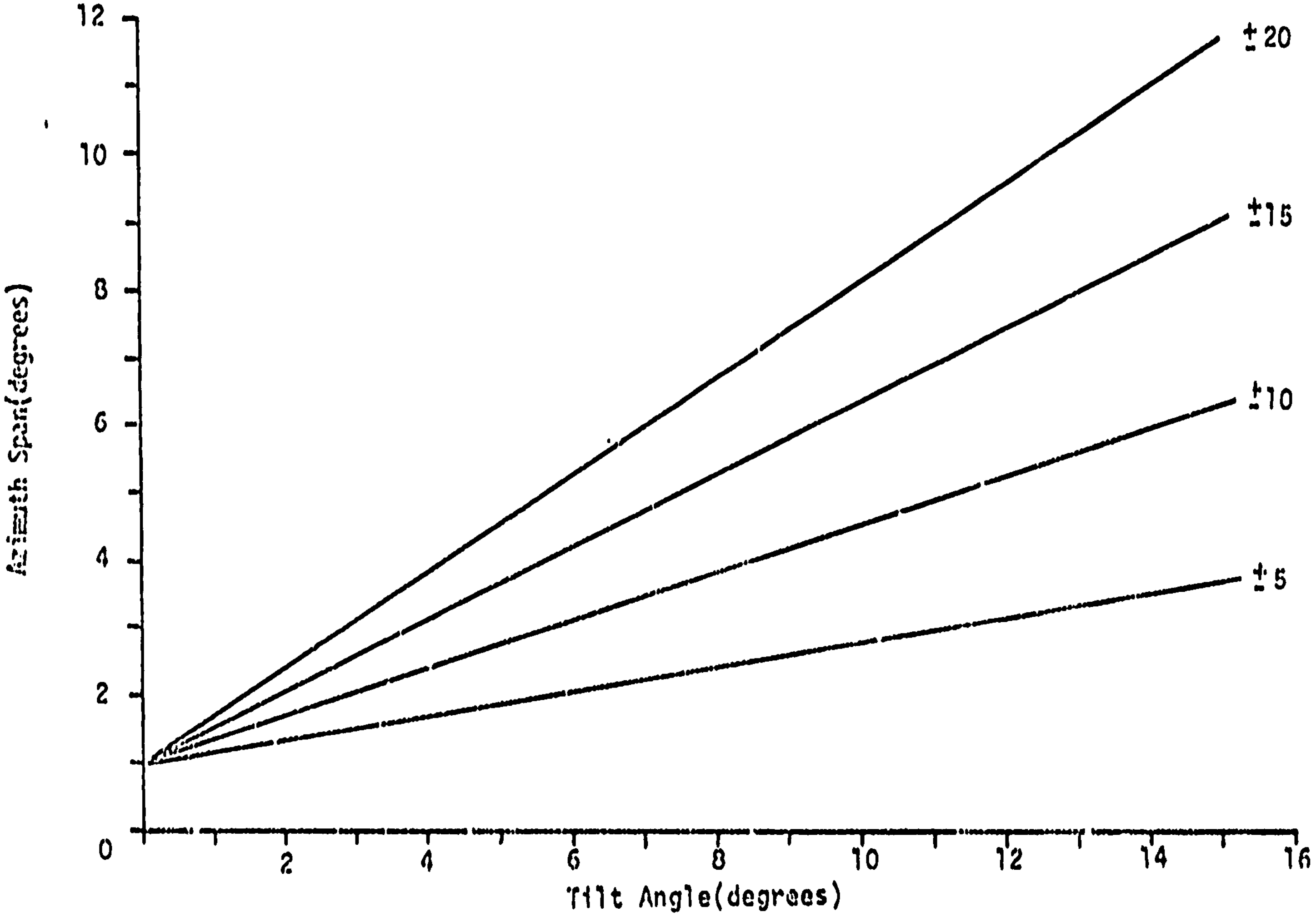

Figure 6. Azimuth Span of Tilted 1° Beam (U)

BEAM NOISE MODEL (U)

(U) Surface ships are the major contributor to the ambient noise background at the frequencies of interest, and will be the only noise sources considered in this study. Energy from surface ships can enter the deep sound channel by three processes:

- o Injection at the edge of the sound channel,
- o Downslope conversion, and
- o Half-channel conversion.

(U) Surface ship energy can be injected into the deep sound channel at the sound channel edge by leakage from the surface duct. This energy enters the sound channel at 0^0 elevation angle; its elevation angle within the deep sound channel is determined by Snell's law. Energy entering the deep sound channel in this way will subsequently appear as a spike at φ where φ varies with range and is determined by Snell's law as shown in Figure 7.

(U) When a surface ship is located over a sloping bottom, energy from the surface ship can be bottom-reflected (with the angle of reflection equal to the angle of incidence), thereby diverting energy into the deep sound channel. This energy will be distributed in elevation angle between $\pm\alpha$ as shown in Figure 8.

(U) In the northern portions of EASTPAC where the axis of the deep sound channel comes to the surface, the major propagation mode is half-channel propagation. As sound energy propagates southward, and as the axis of the sound channel deepens, this half-channel energy is converted to deep sound channel energy distributed between $\pm\alpha$ as shown in Figure 9.

(U) Vertical arrival structure data from CHURCH ANCHOR show that the deep sound channel energy is distributed relatively uniformly within an elevation band of approximately $\pm 15^0$ from the axis of the deep sound channel, which is consistent with both half channel and downslope conversion of energy into the sound channel. (Wagstaff's horizontal directionality studies suggest that most of the energy in the deep sound channel is derived from downslope conversion.)

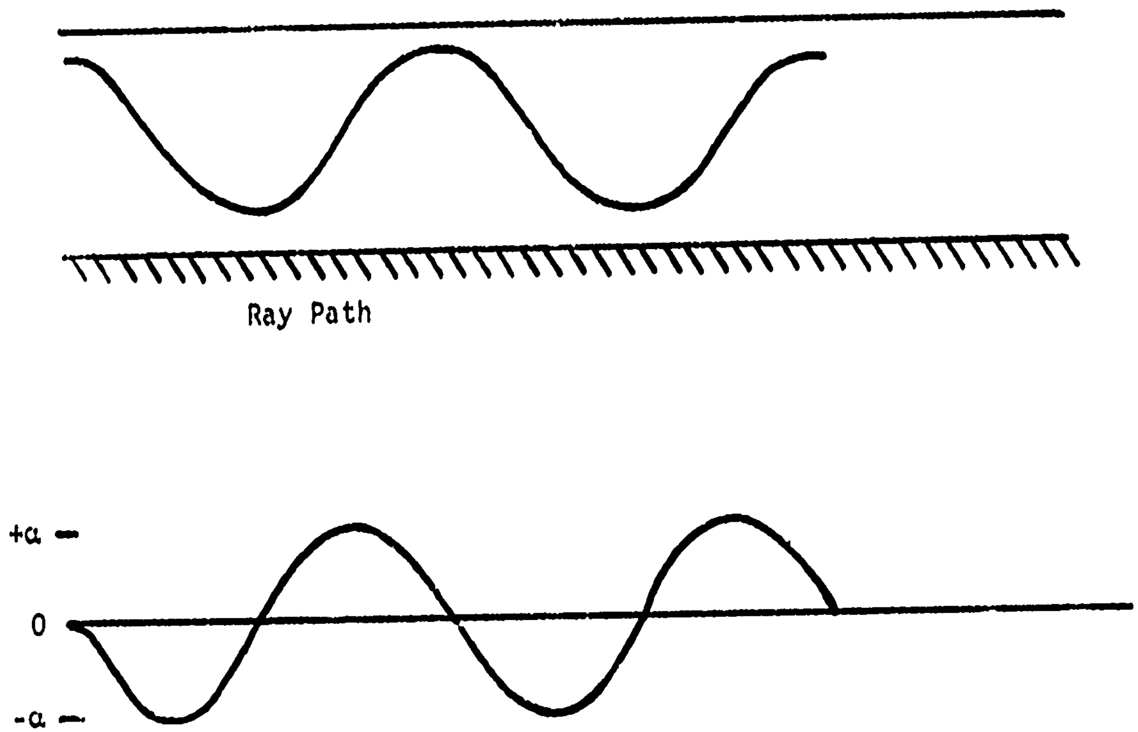

Figure 7. Injection of Energy at Edge of Sound Channel (U)

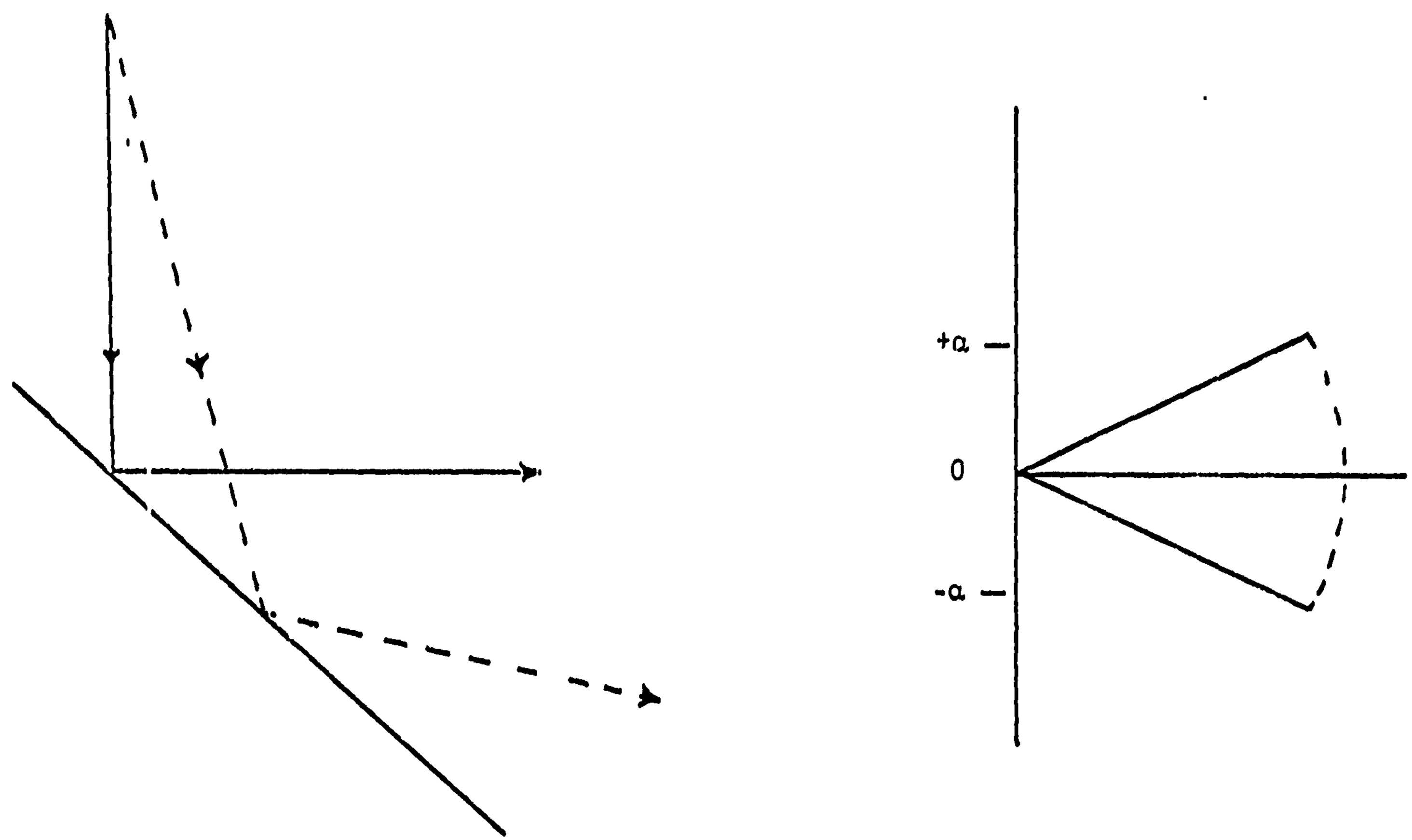

Ray Paths

Energy Distribution

Figure 8. Downslope Conversion of Energy into Sound Channel (U)

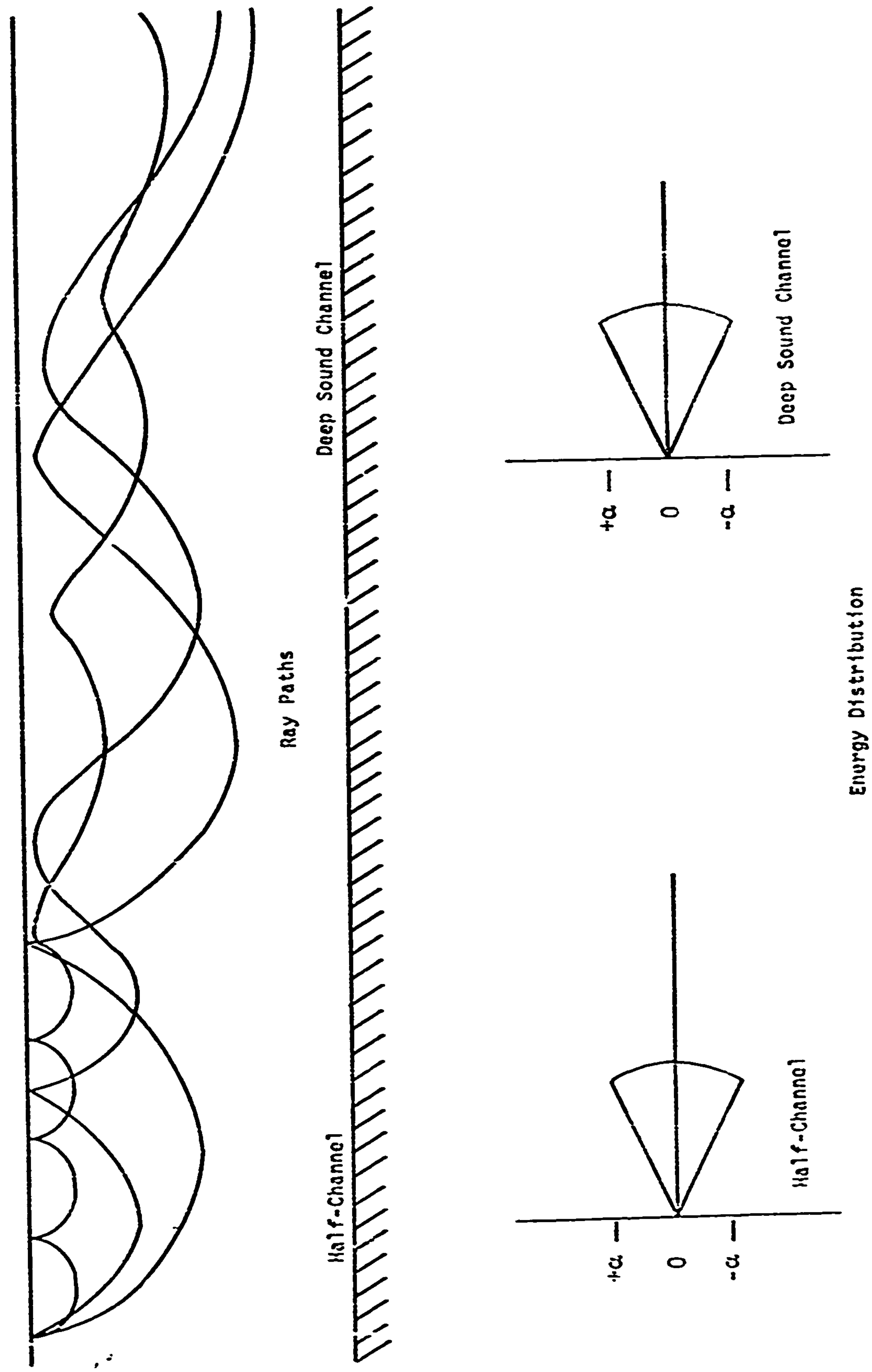

Figure 9. Half-Channel Conversion of Energy into Sound Channel (U)

(U) For EASTPAC conditions, the noise from the distant shipping is uniformly distributed between $\pm\alpha$ (limiting angles) in elevation. When the array is located at the axis of the sound channel, distant shipping noise energy will appear uniformly between $\pm 15^0$; when the array is displaced from the axis of the sound channel (towards the edges), distant shipping noise will be confined between angles equal to the limiting rays.

(C) The beam noise depends on the number of ships on the beam. To determine probability of s ships appearing on the beam, consider the ocean area from which the beam receives energy to be made up of n segments, each having an area ΔA. The density of the ships is taken as ρ, and the probability of a ship appearing in a segment of area ΔA, is equal to $\rho\Delta A$. Since there are n segments in the beam, the probability of s ships appearing on the beam is equal to

$$P(s) = \frac{n!}{s!(n-s)!} (\rho\Delta A)^s (1-\rho\Delta A)^{n-s},$$

the binomial distribution for s "successes" in n independent "trials." In the limit as ΔA becomes small, the binomial distribution becomes Poisson, and hence, the probability of s ships appearing on the beam is equal to

$$P(s) = \frac{e^{-(\rho A)} (\rho A)^s}{s!} .$$

Where the area "covered" by the ideal beam is given by

$$A = \frac{\pi R^2 \theta}{360^0}$$

in which R is the "range" of the beam and θ is the beamwidth.

(C) Figure 10 shows the probability distribution of a number of ships appearing on 1^0, 2^0, 4^0, and 8^0 beamwidth beams for a beam "range" of 1955 nm and an EASTPAC ship density ρ of 3×10^{-5} ships per square nm.

(U) Figure 11 shows a possible distribution of energy from surface ships in azimuth-elevation space. The energy from each ship is distributed uniformly in elevation between $\pm\alpha$ at discrete azimuths realized from the Poisson distribution.

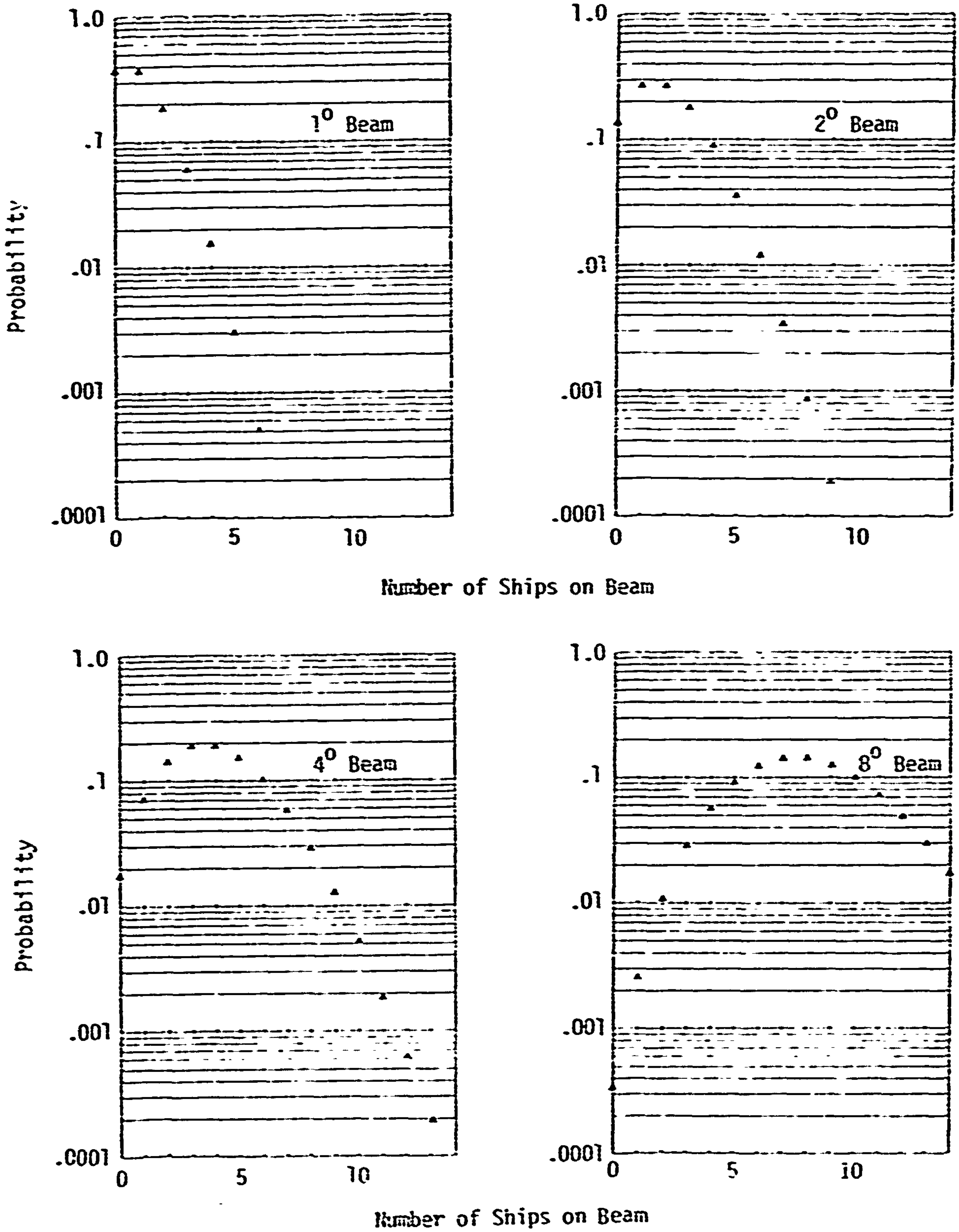

Figure 10. Probability of X Ships on a Beam (U)

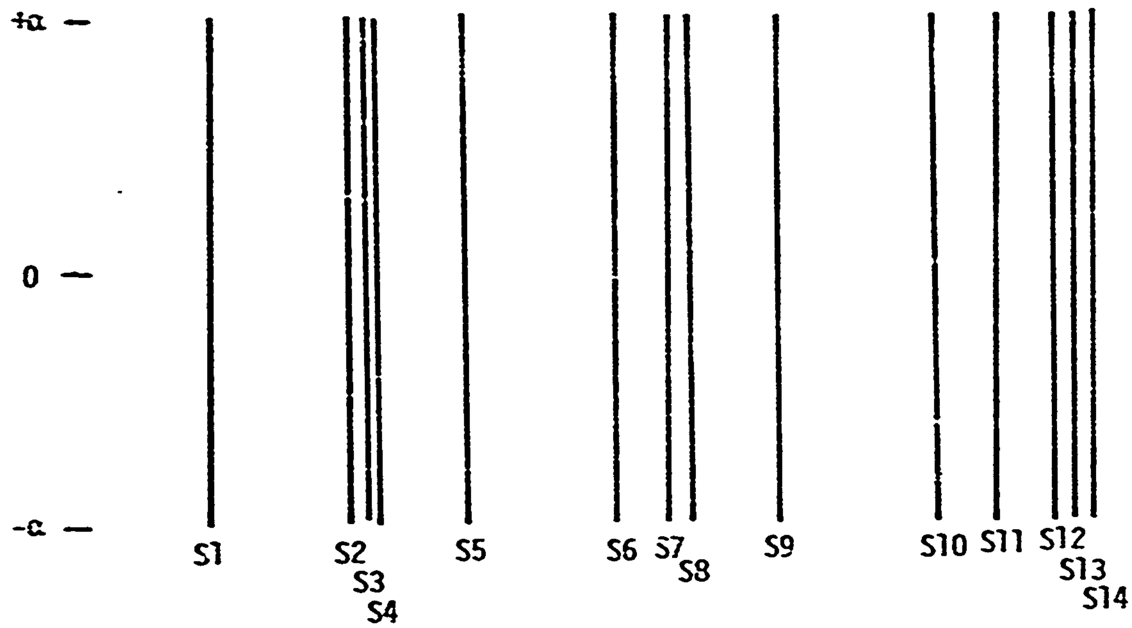

Figure 11. One Possible Azimuth-Elevation Distribution of Energy from Ships (U)

(U) Figures 12A and 12B show how near-broadside beams from a horizontal array and a tilted array, respectively, might sample the ship distribution of Figure 11. Table A presents a tabulation of the ships seen on each beam.

(U) For the array horizontal, each ship appears on only one beam; for the array tilted, each ship can appear on several beams. Thus, in the case of the tilted array, energy from each ship can be distributed over a number of beams.

(U) On the average, a beam will receive a portion of the energy from each ship given by

$$\bar{E} = \frac{\theta}{\theta + 2\alpha \tan \hat{\rho}} E_s,$$

where

$\bar{E}$ = average energy from the ship,
E_s = energy from the ship,
θ = beamwidth,
α = limiting elevation angles, and
$\hat{\rho}$ = array tilt angle

Similarly, the number of ships expected to appear on the tilted beam is

$$s = \frac{(\theta + 2\alpha \tan \hat{\rho})}{\theta} N_o,$$

where

N_o = expected number of ships on a horizontal beam of width θ.

Hence, if on the average, the total energy received from each ship is the same, the mean noise level for a beam will be the same either for the array horizontal or tilted.

(C) Figure 13 shows the cumulative probability that the beam noise level will exceed the levels specified as a function of array tilt, where 0 dB corresponds to the mean noise level. Because of the use of discrete ships and average radiated noise levels, the probabilities are only defined at

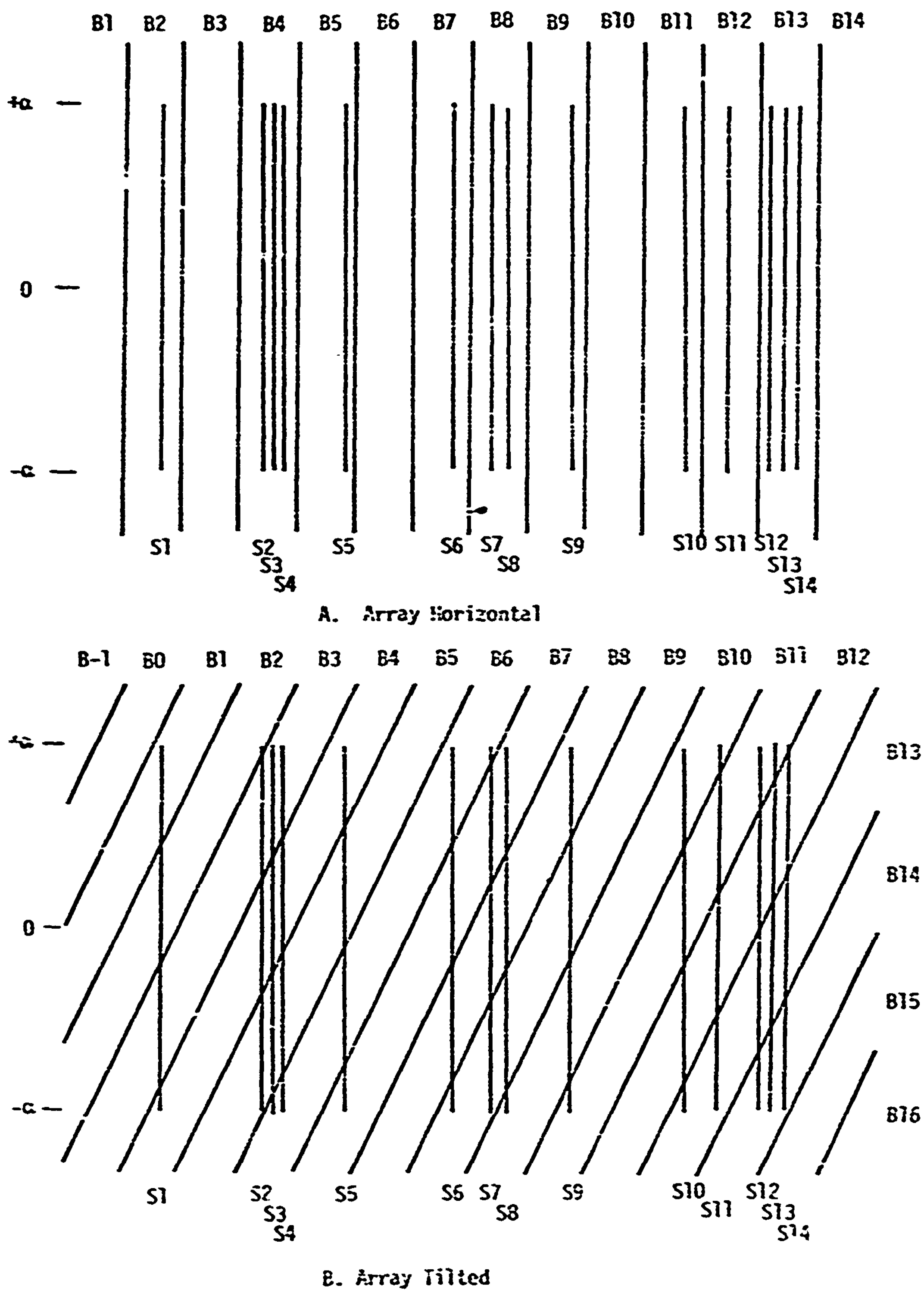

Figure 12. Array Sampling One Possible Azimuth-Elevation Distribution of Energy from Ships (U)

Table A. Beam Ship Counts for Horizontal and Tilted Arrays (U)

Beam	Array Horizontal	Array Tilted
B-1	No data	Incomplete data
B0	No data	Incomplete data
B1	No ships	S1 Incomplete data
B2	S1	S1, S2 Incomplete data
B3	No ships	S1, S2, S3, S4
B4	S2, S3, S4	S1, S2, S3, S4, S5
B5	S5	S2, S3, S4, S5
B6	No ships	S3, S4, S5, S6, S7
B7	S6	S5, S6, S7, S8
B8	S7, S8	S6, S7, S8, S9
B9	S9	S6, S7, S8, S9
B10	No ships	S8, S9, S10, S11
B11	S10	S9, S10, S11, S12, S13
B12	S11	S10, S11, S12, S13, S14
B13	S12, S13, S14	S10, S11, S12, S13, S14 Incomplete data
B14	No ships	S12, S13, S14 Incomplete data
B15	No data	S14
B16	No data	Incomplete data

CONFIDENTIAL

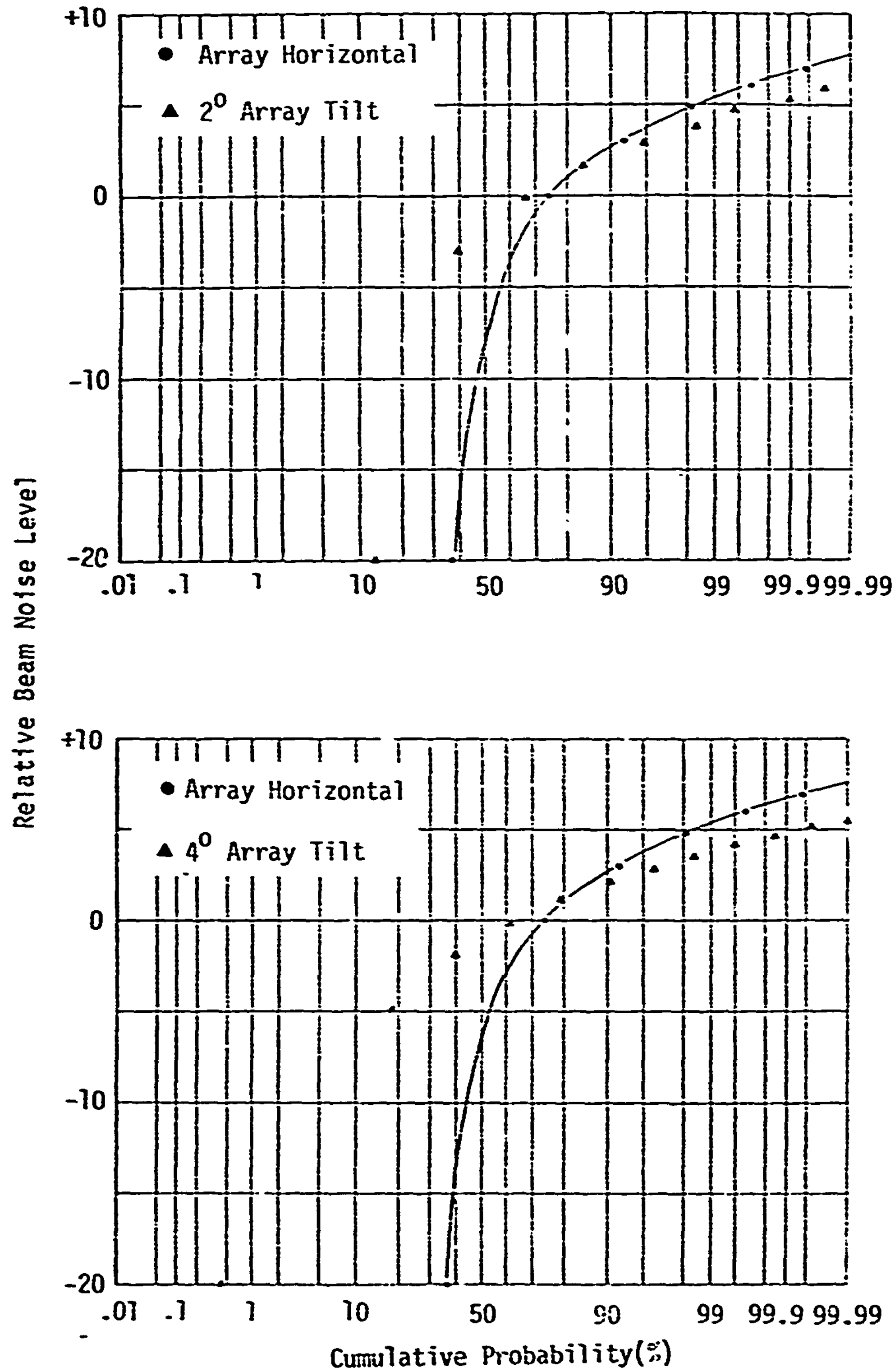

Figure 13. Cumulative Probability of Beam Noise (U)

CONFIDENTIAL

discrete points. The lines connecting the points in Figure 13 are only a guide and are not meant as an interpolation. From these curves, we observe that the probabilities of both very quiet periods and very noisy periods decrease with array tilt.

SIGNAL-TO-NOISE RATIO MODEL (U)

(U) The signal-to-noise ratio model emplcys the beam noise model and a signal model consisting of a discrete source that either injects energy at the edge of the sound channel or is located within the sound channel. When the source injects energy at the edge of the sound channel, this energy will appear at a single elevation angle as determined by Snell's Law and the sound speeds at the channel edge and at the receiver. When the source is located within the sound channel, the energy will be distributed in elevation between angles α and φ where

$$\alpha = \cos^{-1}\left(\frac{C_r}{C_e}\right),$$

and

$$\varphi = \cos^{-1}\left(\frac{C_r}{C_s}\right),$$

in which

C_r = sound speed at the receiver,

C_e = sound speed at the edge of the sound channel, and

C_s = sound speed at the source.

When the sound speed at the receiver is greater than or equal to the sound speed at the source, β is equal to zero and the energy is distributed between $\pm\alpha$.

(C) When the source is within the sound channel, some loss of signal occurs as the array tilts; this loss becomes small, however, as the source approaches the edge of the sound channel. Figure 14 shows the cumulative probability that the signal-to-noise ratio will exceed a specific value as

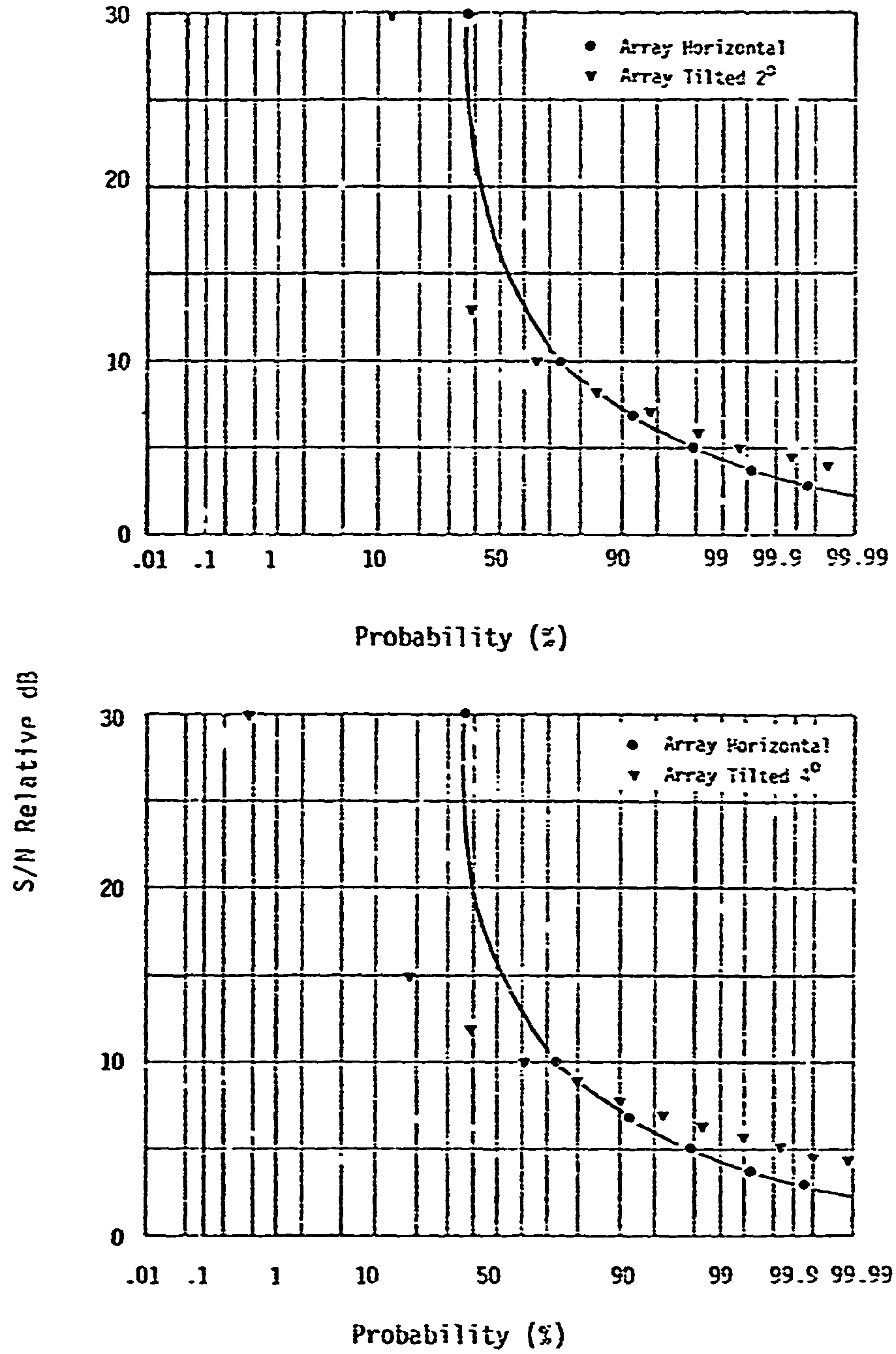

Figure 14. Cumulative Probability that S/N is ≥ Given Value (U)

a function of array tilt when no loss of signal is assumed and when the signal-to-noise ratio of 0 dB is an arbitrary reference level. From these curves it is apparent that high signal-to-noise ratios occur less frequently as the array tilts.

(C) Consequently, if detection opportunities occur when the signal-to-noise ratio is high (corresponding to zero ships on the beam, for example), the probability of detection opportunity occurrence decreases with array tilt as shown in Figure 15.

DETECTION OPPORTUNITY DURATION AND WAITING TIME MODEL (U)

(U) The Detection Opportunity Durati n and Waiting Time Model employs a Markov process of two, and only two, states: zero ships on the beam and one or more ships on the beam.

(C) At any time, the probability of zero ships on the beam is given by

$$P_o = e^{-A\rho}$$

where

$$A = \pi r^2 \frac{(\theta + 2\alpha \tan \beta)}{360^\circ},$$

r = "range" of the beam,
θ = beamwidth,
α = limit ray elevation angle,
β = array tilt angle, and
ρ = shipping density.

The probability of one or more ships on the beam is one minus the probability of zero ships on the beam.

(C) Once there are zero ships on the beam, the system will remain in this state until one or more ships enter the beam, where the probability of one or more ships entering the beam in a time interval, Δt, is

$$P_o(\Delta t) = 1 - e^{-\rho r s \Delta t}$$

in which

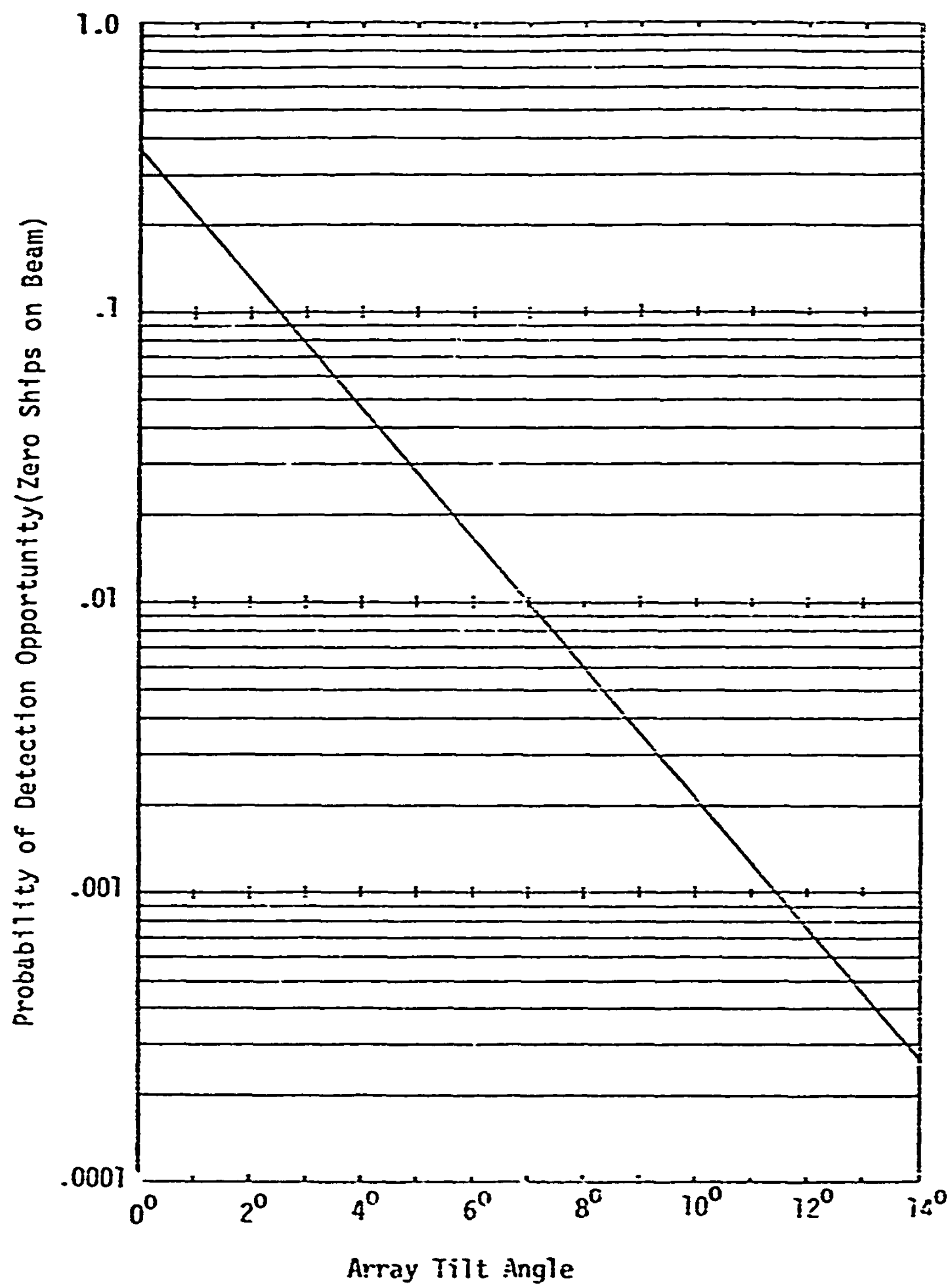

Figure 15. Probability of Detection Opportunities (U)

p = shipping density,

r = "range" of the beam, and

s = average of the component of ship speeds perpendicular to the axis of the beam.

If we assume an average of the component ship speeds perpendicular to the axis of the beam equal to 15 knots and, as before, a beam "range" equal to 1955 nm and a shipping density ρ of 3×10^{-5} ships per square nm, the average time required for one or more ships to enter the beam is equal to 47.3 minutes, which is independent of array tilt.

(C) It can be shown that the average waiting time between periods of zero ships on the beam is equal to the average period of one or more ships on the beam, and is given by

$$T_W = T_H \frac{P_{\geq 1}}{P_0},$$

where

T_W = Average waiting time between periods of zero ships,

T_H = Average period for zero ships,

P_0 = Probability of zero ships on the beam, and

$P_{\geq 1}$ = Probability of one or more ships on the beam and is equal to $1 - P_0$.

(U) Figure 16 shows waiting times for a beam of 1^0 width as a function of array tilt for limiting ray elevation angles of $\pm 7.5^0$, $\pm 10^0$, and $\pm 15^0$.

SUMMARY OF RESULTS (U)

(C) The models developed for and employed in this study indicate that some performance measures are independent of array tilt, whereas others are sensitive to array tilt. We have shown that the following performance measures are independent of array tilt:

- Mean Beam Noise Level - Independent of array tilt but increasing with increasing beamwidth and shipping density,

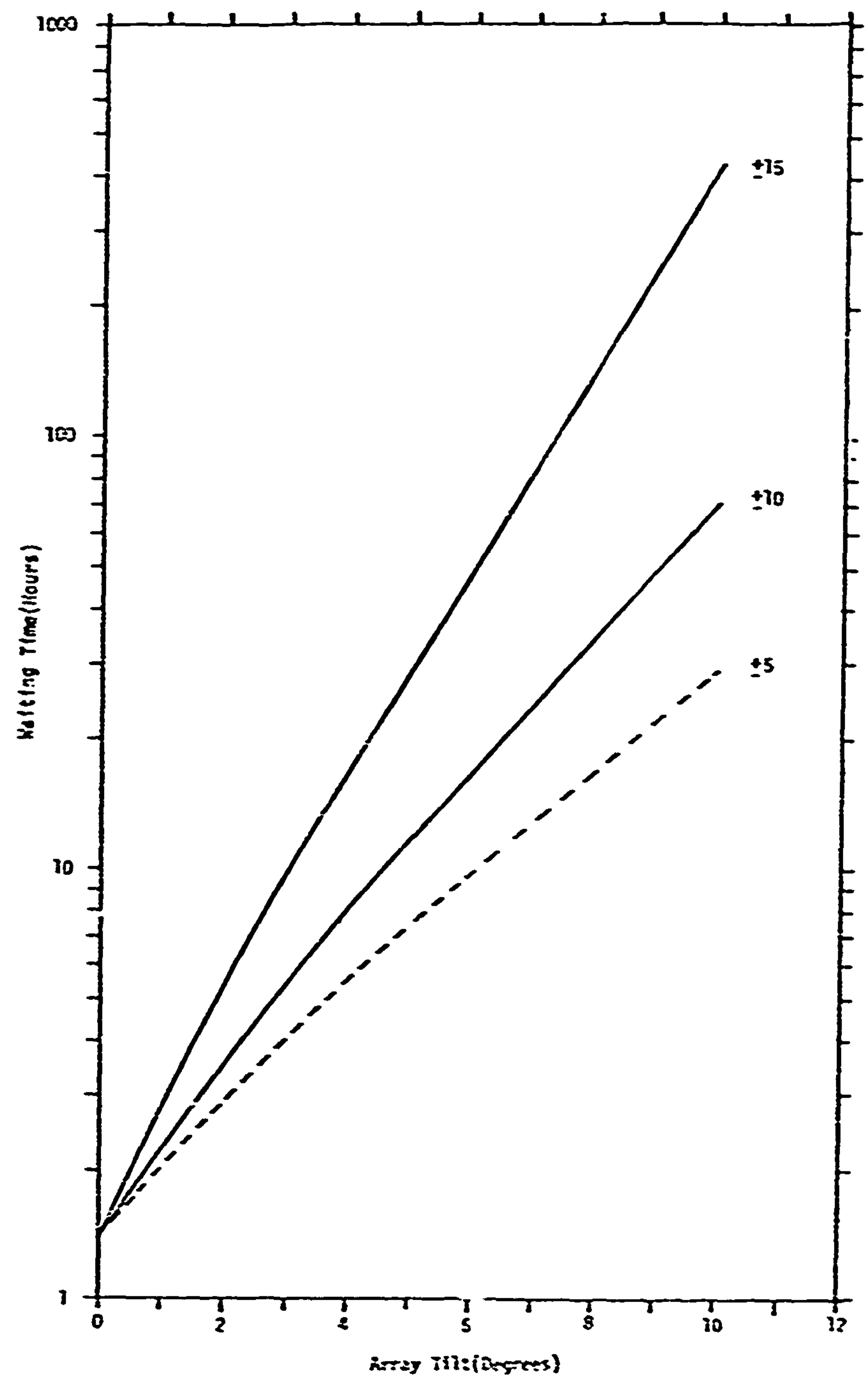

Figure 16. Waiting Times Between Detection Opportunities (U)

- o Mean Signal-to-Noise Ratio - Independent of array tilt but decreasing with increasing beamwidth and density, and
- o Mean Duration of Detection Opportunities - Independent of array tilt and beamwidth but decreasing with increasing shipping density and average ship speed.

(C) We have also shown that the following performance measures are sensitive to array tilt:

- o Beam Noise Fluctuations - Variance decreases with array tilt and increasing beamwidth and shipping density,
- o Signal-to-Noise Ratio Fluctuations - Variance decreases with array tilt and increasing beamwidth and shipping density,
- o Probability of Detection Opportunities (zero ships on the beam) - Decreases with array tilt and increasing beamwidth and shipping density,
- o Mean Waiting Time Between Detection Opportunities (zero ships on the beam) - Increases with array tilt, increasing beamwidth and shipping density, and decreasing average ship speed.

(U) These trends are independent of the specific values of beamwidth, shipping density, and average ship speed used in the computations.

CONCLUSIONS (U)

(C) The detection performance of a line array system degrades as the array tilts from the horizontal plane. An array tilt of approximately 1.5^{0} on an array having 1^{0} beams operating at the axis of the sound channel reduces the probability of obtaining a detection opportunity to one-half the value for a horizontal array.

(C) As the array tilts, the observation time required to obtain meaningful estimates of beam noise and signal-to-noise ratio statistics increases. Where meaningful estimates may be obtained in 10 to 20 hours on a horizontal array, 50 to 100 hours are required when the array tilts 3^{0} from horizontal.

ACKNOWLEDGEMENTS (U)

(U) The author wishes to express his appreciation to his colleagues at Xonics. He is particularly grateful to Drs. James H. Wilson and Wentworth Williams for extensive discussions that were most useful in the development of these models. He is also grateful to W. Paul Jameson, Scott C. Daubin, Jr., and Sherrill Potts for their assistance in the preparation of this manuscript, and to Isabelle Lipson who typed this manuscript.

DEPARTMENT OF THE NAVY
OFFICE OF NAVAL RESEARCH
875 NORTH RANDOLPH STREET
SUITE 1425
ARLINGTON VA 22203-1995

IN REPLY REFER TO:

5510/1
Ser 321OA/011/06
31 Jan 06

MEMORANDUM FOR DISTRIBUTION LIST

Subj: DECLASSIFICATION OF LONG RANGE ACOUSTIC PROPAGATION PROJECT (LRAPP) DOCUMENTS

Ref: (a) SECNAVINST 5510.36

Encl: (1) List of DECLASSIFIED LRAPP Documents

1. In accordance with reference (a), a declassification review has been conducted on a number of classified LRAPP documents.

2. The LRAPP documents listed in enclosure (1) have been downgraded to UNCLASSIFIED and have been approved for public release. These documents should be remarked as follows:

   Classification changed to UNCLASSIFIED by authority of the Chief of Naval Operations (N772) letter N772A/6U875630, 20 January 2006.

   DISTRIBUTION STATEMENT A: Approved for Public Release; Distribution is unlimited.

3. Questions may be directed to the undersigned on (703) 696-4619, DSN 426-4619.

BRIAN LINK
By direction

Subj: DECLASSIFICATION OF LONG RANGE ACOUSTIC PROPAGATION PROJECT (LRAPP) DOCUMENTS

DISTRIBUTION LIST:

NAVOCEANO (Code N121LC – Jaime Ratliff)
NRL Washington (Code 5596.3 – Mary Templeman)
PEO LMW Det San Diego (PMS 181)
DTIC-OCQ (Larry Downing)
ARL, U of Texas
Blue Sea Corporation (Dr.Roy Gaul)
ONR 32B (CAPT Paul Stewart)
ONR 321OA (Dr. Ellen Livingston)
APL, U of Washington
APL, Johns Hopkins University
ARL, Penn State University
MPL of Scripps Institution of Oceanography
WHOI
NAVSEA
NAVAIR
NUWC
SAIC

Declassified LRAPP Documents

Report Number	Personal Author	Title	Publication Source (Originator)	Pub. Date	Current Availability	Class.
TIRC1871976F	Hoffmann, J., et al.	CHURCH ANCHOR AMBIENT NOISE FINAL REPORT (U)	Texas Instruments, Inc.	750901	ADC070512; NS; AU; ND	C
Unavailable	Unavailable	SQUARE DEAL ANALYSIS EXECUTIVE SUMMARY (U)	University of Texas, Applied Research Laboratories	751001	AU	C
Unavailable	Unavailable	SQUARE DEAL ENVIRONMENTAL ACOUSTIC SUMMARY SEC. IV-SIGNAL PROPAGATION (U)	Xonics, Inc.	751101	AU	C
Unavailable	Unavailable	CHURCH ANCHOR CW PROPAGATION LOSS AND SIGNAL EXCESS REPORT (U) PRELIMINARY	Texas Instruments, Inc.	751201	AU	C
SAN-BBOP-76-U127. B38485	Unavailable	MSS CONFIGURED ACODAC SYSTEMS FINAL ENGINEERING REPORT (U)	Sanders Associates, Inc.	760115	ND	C
Unavailable	Unavailable	MSS CONFIGURED ACODAC SYSTEMS PRELIMINARY TEST REPORT-BEARING STAKE (U)	Sanders Associates, Inc.	761111	AU	C
ARL-TR-76-52	Watkins, S. L.	MOORED SURVEILLANCE SYSTEM FIELD VALIDATION TEST AMBIENT SOUNDFIELD AND PROPAGATION MEASUREMENTS FOR NEAR-BOTTOM SENSORS AT SITE A3 (U)	University of Texas, Applied Research Laboratories	761201	ND	C
Unavailable	Unavailable	REAL-WORLD MEASUREMENTS Of MSS ACODAC HYDROPHONE RESPONSE PATTERNS (U) PHASE REPORT - PRELIM DRAFT	Naval Air Development Center	761222	AU	C
XONICSTR109OSD	Morey, C. F.	EFFECT OF ARRAY TILT ON BEAM NOISE, SIGNAL-TO-NOISE RATIO, AND DETECTION OPPORTUNITY	Xonics, Inc.	770101	NS; ND ADC010061	C
NRL-7996	Andriani, C. R., et al.	ACOUSTIC PROPAGATION IN THE LABRADOR SEA	Naval Research Laboratory	770308	ND	C
Unavailable	Gabrielson, T. B.	REAL-WORLD MEASUREMENTS Of MSS ACODAC HYDROPHONE RESPONSE PATTERNS	Naval Air Development Center	770601	ADC010980	C
NAVSO P970V27, NO. 3	Del Balzo, D. R.	TOWED ARRAY DYNAMICS AND ACOUSTIC IMPLICATIONS (U)	Office of Naval Research	770701	ND	C
WHOI-77-55	Baxter, L.	MSS-FVT ACODAC DATA ASSESSMENT AND AMBIENT NOISE THIRD OCTAVE DATA PROCESSING (U)	Woods Hole Oceanographic Institution	770801	AU; ND	C
Unavailable	Unavailable	LARGE APERTURE MARINE BASIC DATA ARRAY (LAMBDA) SYSTEM DESCRIPTION	Naval Ocean R&D Activity	770901	AU	C
Unavailable	Unavailable	CHURCH STROKE REVIEW (U)	University of Texas, Applied Research Laboratories	770912	AU	C
NOSCTR169	Yee, G. S.	BEARING STAKE EXERCISE PRELIMINARY RESULTS (U) RESEARCH AND DEVELOPMENT REPORT OF JAN-MAY 77	Naval Ocean Systems Center	771031	NS; AU; ND	C
LRAPPRC77020	Palumbo, J. X., et al.	LRAPP EXERCISE ACOUSTIC DATA INVENTORY DECEMBER 1977 (U)	Naval Ocean R&D Activity	771201	NS; ND	C